Trans. JSASS Aerospace Tech. Japan
Vol. 19, No. 3, pp. 310-318, 2021
DOI: 10.2322/tastj.19.310

High-School CanSat Model for Advancement of Agricultural Process in Thailand

By Bhavat NGAMDEEVILAISAK[1)], Chayakorn VONGBUNSIN[1)], Chayanin UTHANPATHUMROS[1)], Vivatsathorn THITASIRIVIT[1)], Phachara PHUMIPRATHET[1)] and Peeramed CHODKAVEEKITYADA[2)]

[1)]*A.E.A. Sat Team, Assumption College, Bangkok, Thailand*
[2)]*Faculty of Engineering, King Mongkut's Institute of Technology Ladkrabang, Bangkok, Thailand*

(Received June 26th, 2019)

Thailand's agriculture is economically remarkable but most of agriculturists and farmers, on the contrary, have significantly low profit. Nowadays, technology is used to solve many agricultural problems, especially analyze area to find the most suitable crops and area for efficient growth rate of crops. Agricultural Exploration Assistant Satellite or AEASat is the CanSat prototype that participated in Thailand CanSat Competition 2018 and received The First Place Winner and The Best Presentation Awards. The goals of AEASat are to study environmental growth factors (temperature, relative humidity, average rainfall, carbon dioxide intensity, red and blue light intensity) of six Thai economic crops (rice, cassava, maize, sugarcane, rubber tree, palm) and find the most suitable area for many agricultural actions. The first mission of AEASat takes place in Chai Badan, Lop Buri Province, Thailand. Electronic structure of AEASat is categorized into four floors respect to their functions: sensors floor, main controller floor, data logger and wireless communication floor, and power management floor. Another part of the mission is the ground unit. The ground unit also collects environmental factors including light intensity which AEASat does not collect. The last part of the mission is ground station. The function of the ground station is receiving data from AEASat with wireless 488-MHz-frequency LoRa module. The ground station is also used to track AEASat from deployment to a touchdown. Qualitative data and quantitative data are analyzed with different methods. The qualitative data is evaluated to find the growing suitability in the area by using Geographic Information System (GIS) software. Aerial photograph, a part of qualitative data, is analyzed by visual interpretation. The quantitative data is analyzed by calculating average of the correlation coefficients of six factors by using MATLAB. It is calculated in order to find the most suitable crop out of six to grow in the area. As a result, sugarcane is the most suitable crop to grow in Chai Badan area. Agriculturists and farmers can have access to website which the results, detail, and description of the exploration are uploaded. In conclusion, if agriculturists and farmers grow the crops as advised, they can expect more products quantity.

Key Words: AEASat, CanSat, Economic Crops, Geographical Information System, Ground Unit

Nomenclature

A	:	surface area, square meter
AEASat	:	Agricultural Exploration Assistant Satellite
GIS	:	geographical information system
GPS	:	Global Positioning System
g	:	acceleration due to gravity, meter per second squared
MC	:	main controller
m	:	mass, kilogram
N	:	number of samples
PCB	:	printed circuit board
R.S.	:	relative suitability
t	:	time, second
v	:	velocity, meter per second
x	:	position from start, meter
ρ	:	air density, kilogram per cubic meter

1. Introduction

Thailand CanSat Competition 2018 is a national CanSat competition for high-school students. It was held to develop students' ability based on Science, Technology, Engineering, and Mathematics Education (STEM Education) in Thailand. CanSat competition is also a project-based learning. There were 80 teams participated in this competition and only 10 teams were chosen for the final round competition in December. Our team got into the final round and got 2 prizes: The First Place Winner Awards and The Best Presentation Awards.

Agriculture in Thailand is quite remarkable. Thailand is designated as 'The Kitchen of The World.' Thai farmers' income is relatively low to average income of Thai people (57,032 Baht/year to average of 320,000 Baht/year). In addition to the income data, 40 percent of Thai farmers are below the poverty threshold. Our group was aware of this problem and created solutions to solve it.

Agricultural Exploration Assistant Satellite (AEASat) is one of the CanSat models which is aimed to help exploring land area that has the most suitability—positively influences the growth of economic crops. The process of exploring land might be a difficult and time-consuming action without help of technology. Nowadays, the computer and technology are very advanced and take less effort for some actions that human can hardly do it alone. On the other hand, the cost of human resource would be higher than using computer to collect and process data in a long-term use. A number of farmers can hardly access most useful information; thus, some crops would not be efficient and effective for growing in the specific area.

The missions of AEASat has two parts. Main mission is to collect physical data—atmospheric temperature, humidity, carbon dioxide intensity, average annual rainfall, red and blue light intensity—from atmosphere and databases to be numerically processed and decide the crops suitable for growing in the study area is. Secondary mission is to use the following quantitative parameters to visualize those factors collected in the study area and find the most suitable subarea to grow crops using averaging and data interpolation to perform a spatial analysis method and create a map. The visual interpretation is also used for analyzing the aerial photography. AEASat had the first launch in Chai Badan, Lop Buri Province, Thailand, descended from the 350-metre-height through about 50 kilometers per hour wind speed in the air.

2. Mechanical Design

2.1. Enclosure and internal compartment design

Because electronic components are fragile, and vulnerable to shock, vibration and instantaneous impact; those components need to be protected. The electronic circuits of the system are designed as stacked PCBs because the space inside the enclosure can be efficiently managed to be as compact as possible. Those PCBs are loosely connected by 4 stainless steel rods which act as main pillars and separated by plastic straws to prevent any metal contacts with the circuit which can lead to a circuit short and system failure due to the hardware. The metal springs were also used at the end of each pillar to absorb the force during impact on a touchdown. In addition to the spring-structural supports, the supportive sponge is added above the bottom lid to reduce the impact force along with the existing springs. Overall schematic of AEASat is shown in Fig. 1. Furthermore, the connected internal components are externally protected by specially designed 3D printed shell and lids using Polyethylene terephthalate (PETG) plastic material as printing filament. PETG plastic is equivalent to Polycarbonate (PC) plastic. The physical structure of PETG plastic is rigid but it has special property: flexible structural components, it reduces the fragility of the enclosure and reduces the probability of fracture after impact, so our both AEASat electronic components and mechanical protective layer is fully reusable.[2] The shell is designed to increase the airflow intensity and laminar airflow, and to reduce the turbulence airflow during descent which can lead to unstable and shaky descending and causes blurry aerial images. On descent, AEASat do not descend with the body perpendicular to ground but slightly tilted to reduce turbulence flow in addition to the shell design. Both lids are designed to include holes for inserting tight and sturdy stainless-steel pillars and also include a camera cutout in the bottom lid for Raspberry Pi Camera to capture images below AEASat. With all the mechanical protection, it will have rigid, strong and flexible structure. The final dimension of AEASat has the diameter of 68 millimeters and the height of 140 millimeters. Before testing the structure, we simulated the force which impacted the AEASat when the internal components are loaded. The simulation result is illustrated in Fig. 2.

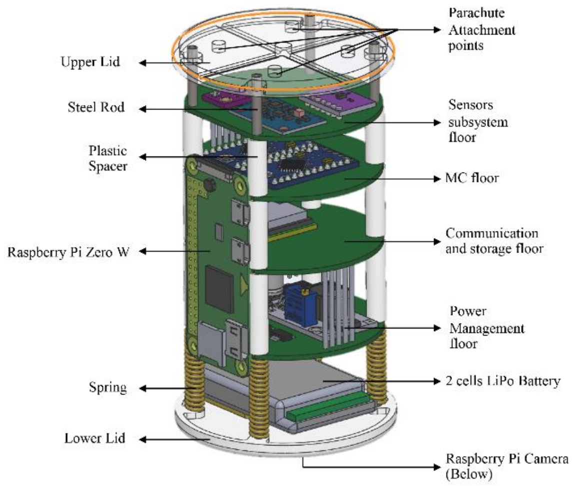

Fig. 1. The overall physical layout 3D model schematics of AEASat.

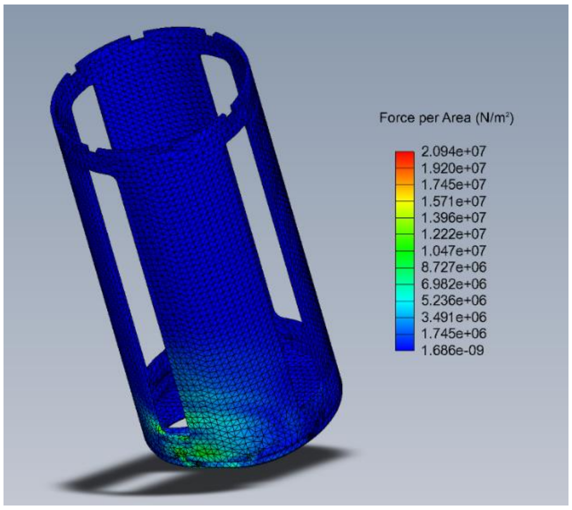

Fig. 2. Force (Von Mises stress) on instantaneous impact simulated by SOLIDWORKS 3D stress simulation.

2.2. Parachute design

AEASat starts descending from the height of 350 meters; thus, the touchdown without any slowdown would cause instantaneous impact and ultimately damage the components. For those reasons, we decided to use a parachute to slowdown the terminal velocity of descent for reducing the impact force on a touchdown. For the calculation of the size of parachute, the drag equation was used.[1)] The motion with drag equation in integral form was derived as shown in Eq. (1):

$$\int_{t=0}^{t} \mathrm{d}t = \int_{v_i=0}^{v(t)} \frac{1}{g - \frac{k}{m}v^2} \mathrm{d}v \,, \tag{1}$$

into $v(t)$ and $x(t)$ equations as shown respectively in Eqs. (2) and (3):

$$v(t) = \sqrt{\frac{mg}{k}} \tanh\left(t\sqrt{\frac{gk}{m}}\right), \tag{2}$$

and

$$x(t) = \frac{m}{k} \ln\left\{\cosh\left(t\sqrt{\frac{gk}{m}}\right)\right\}, \tag{3}$$

where

$$k = \frac{1}{2}\rho_{atm} c_d A \,. \tag{4}$$

The type of parachute we chose is round-type with an air vent in the middle. Because round-type parachute has relatively high forward speed, the coverage of study area of our mission would be higher. On the contrary, this type of parachute has high turbulence airflow during perpendicular wind impact on the parachute surface, so the middle air vent is added to the design in order to increase the laminar airflow. The area of the air vent to the parachute body has a ratio of about 8 percent. Added to the fact that overall weight of AEASat with a parachute is approximately 290 grams, the terminal velocity—touchdown speed—would be roundly equal to 2.5 meters per second which is safe for future reuses. For ensuring least turbulence flow, we simulated the airflow around AEASat and parachute with Autodesk Flow Design simulation software. The part of results is shown in Fig. 3. When AEASat was dropped from a 350-meter height, it was dropping flawlessly without turbulence of air.

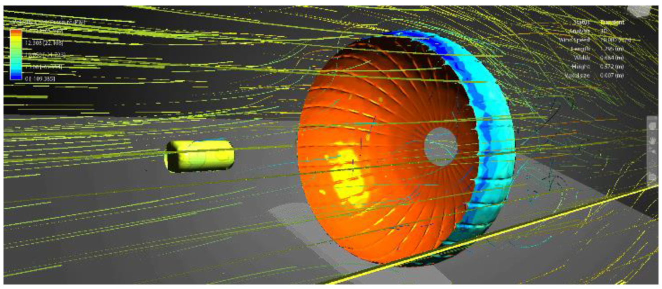

Fig. 3. Parachute airflow simulation.

3. Electronics and Circuit Design

According to our requirements of the mission, we cannot connect all electronic components by wires, so we reduce the wiring process by designing our own circuitry. We chose printed circuit board (PCB) as an option for packing all components as needed and for making AEASat sturdy, solid, tight and as compact as possible. We also chose double-layered PCBs to install our components on both sides of each PCB and use as much space as possible. As mentioned, the stacked PCBs design is used instead of single-board design. All PCBs are connected by power line and communication line in parallel. The floors of AEASat designs and labels are shown in Fig. 4.

As our mission requires a number of electronic components, the way we handle these complications is categorizing those components into 6 parts, allocated by their functions and usages: sensors subsystem floor, main controller floor, communication-and-storage floor, power management subsystem floor, attached camera unit, and ground unit as follows. The first 4 mentioned parts are floors of AEASat, and the ground unit is the additional parts deployed on the field, not implemented on it.

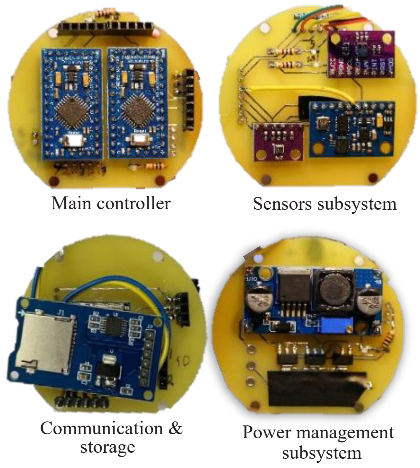

Fig. 4. AEASat floor designs.

3.1. AEASat sensors subsystem floor

The sensors subsystem floor consists of sensor components according to the objectives and data acquisition needs. We designed AEASat to be as compact as possible, packed all the sensors in a floor (2 layers per floor); thus, meets the requirements of the mission. Each PCB has a diameter of 6 centimeters and fits loosely in the AEASat to prevent sturdy impact force. The list of sensors components and their functions is given in Table 1.

Table 1. Sensors components and their functions.

No.	Components	Functions
1.	BME280	Atmospheric relative humidity, air pressure and temperature sensor
2.	CCS811	Carbon dioxide intensity sensor
3.	GY-801	Gyroscopic orientation sensor

3.2. AEASat Main Controller (MC) floor

This floor includes 2 Arduino Pro mini MCs for obtaining data from sensors and processing packets to use in the other parts of the system.

3.3. AEASat communication-and-storage floor

The communication-and-storage floor includes wireless communication module, SD storage module and GPS module. The list of components and their functions is given in Table 2.

Table 2. COM floor components and their functions.

No.	Components	Functions
1.	LoRa RA-02	1-way wireless communication with ground station
2.	Catalex V1.0	MicroSD card data logger
3.	ATGM336H	Retrieving GPS coordinates

3.4. AEASat power management subsystem floor

AEASat needs electrical power management subsystem to maintain the voltage and current of the system. The 3.7 V LiPo battery with capacity of 2,500 mAh was chosen because—as the power drawing of the system was measured, it draws 1.2 A of current at maximum load. The nominal consumption (average) is 830 mA. The margin is LoRa module transmitting data (120 mA) and Raspberry Pi capturing image and saving to SD card (200 mA). The margin includes any power loss due to converted voltage and heat at arbitrary time. As the system needs both 3.3 V and 5 V to operate with different components, the power subsystem shall have XL6009 which steps up the voltage to 5 V and three AMS1117 modules which are connected in parallel to step down the voltage to 3.3 V without overloading the power this module can handle. The safety of the system is highly concerned, TP4056 module helps prevent overcharging and featured with short circuit protection. The module has LED that indicates the battery status on the other side of this floor.

3.5. Attached camera unit

One of the parts of qualitative data is aerial photograph, we need a camera to retrieve that information, so Raspberry Pi is chosen. The Raspberry Pi has faster CPU and image processor clock speed, so the image is processed and logged into memory as it is taken. It uses Raspbian, Debian-based operating system, to operate hence more system efficiency; Arduino could be used to take and process image, but the quality and processing speed is relatively low to Raspberry Pi Zero W—the model we used.

3.6. Ground unit

To increase the accuracy and precision of collected data, more data-collecting unit is required in addition to the existing AEASat. The quantitative data is collected from both parts, and later be used by numerical process. This ground unit collects basic parameters by using sensors as shown in Table 3, but it is also used to collect red and blue light intensity by using GY-9960LLC (red, green and blue spectrum intensity sensor) for the analysis.

Table 3. Ground Unit components and their functions.

No.	Components	Functions
1.	Arduino Uno R3	Main controller of ground unit
2.	BME280	Atmospheric relative humidity, air pressure and temperature sensor
3.	CCS811	Carbon dioxide intensity sensor
4.	Catalex V1.0	MicroSD card data logger
5.	GY-9960	Red, green and blue light intensity detector.

4. Integration Test

After the assembly of AEASat, the after-assembly (integration) test is required. The continuity and reliability of the data is also mandatory. The integration tests we held are wireless communication range and obstruction test, power consumption test, and structure test.

4.1. Sensors test

The sensors functionalities were both individually and integrally tested as stated in Table 4.

Table 4. Sensors individual test.

No.	Components	Tests
1.	BME280	After the I^2C communication is valid, the temperature, pressure, and humidity value are compared with respective analog meters.
2.	CCS811	The reliability of value is validated by comparing with high accuracy sensor from average hourly carbon dioxide intensity.
3.	GY-801	Euler angles measured from the gyroscope are compared with 3-axis level.
4.	ATGM336H	Five to ten coordinates are plotted and compared with real world location.
5.	Catalex V1.0	The continuity test is conducted. The parity is checked for 2 hours of operation.

4.2. Wireless communication range and obstruction test

The major part of CanSat telemetry is wireless communication—either one-way or two-way. Without AEASat-ground station communication, the location of AEASat could not be tracked, and the recovery would be more complicated than it should be. The wireless communication test is held at King Mongkut's Institute of Technology Ladkrabang (KMITL). KMITL is wide and convenient for line-of-sight signal tracking. The illustration of the path we tested is shown in Fig. 5.

Fig. 5. Wireless communication test. Yellow line represents the path we walked from placemark A to C and vice versa.

As shown in Fig. 5, placemark A is where the ground station was placed. We started at the placemark A and slowly walked towards placemark C (the end point of the road). The receiver antenna is directly pointed towards the AEASat. On the road we used to test, there were cars and objects obstructing the line of sight of the communication, so the signal strength is not much degraded from clear line of sight. When we reached placemark B, the signal strength is significantly low. The data packets which is sent by AEASat is started to be unhealthy from the placemark B to placemark C. At placemark C, the signal from AEASat is completely loss and the AEASat cannot communicate with the ground station. After that, we started walking back towards the starting point (placemark A), and then gained some data packets back. The distance of tested path (A to C) was 560 meters and the optimal distance (A to B) was 500 meters.

4.3. Power consumption test

For the power consumption of AEASat test, we measured the duration of power-on state of AEASat with stopwatch. The distance between AEASat and the ground station is 2 meters. If the data packets sent by AEASat are complete, the battery of AEASat is still functional. The battery is not considered functional if the packets are incomplete or not sending.

4.4. Structure test

The final part of testing before the deployment was the structure test. In this section, we tested the enclosure strength, internal compartment protector strength, and parachute. Those tests are performed by dropping AEASat from the top of a five-floor building at Assumption College. The experiment showed that wind affected parachute forward speed more than resisting descending speed, so an eighty-centimeter-diameter circular parachute with a eleven-centimeter-diameter hole is effective for our mission as we needed to cover large area. Another section of this test was structural strength test. We repeatedly dropped AEASat from the building; and then at the 9th time, the enclosure began to shatter. Because of the concrete floor, the impact force might be higher than it could withstand. Most of the study area is grass or plain, so AEASat is reusable in terms of structural strength.

5. Plant Growth Environmental Factors

5.1. Light

Plants need sufficient light source to help the photosynthetic process in order to grow into crops. Each plant has different photosynthetic pathway and different optimal frequency range of light.[3] Commonly, plants are categorized into 3 groups using methods of Calvin cycle in photosynthetic process: C3 plants, C4 plants, and CAM (Crassulacean Acid Metabolism) plants.

About 85 percent of all plant species in nature are C3 plants. They do not have photosynthetic adaptations to reduce photorespiration. In C3 plants, the light-dependent reaction and Calvin cycle occur in the same area, the mesophyll. The mesophyll of the C3 plants are separated into 2 layers: palisade mesophyll and spongy mesophyll. They use only rubisco enzyme for carbon dioxide fixation in the Calvin cycle.

On the contrary to the C3 plants, in C4 plants, the light-dependent reactions and Calvin cycle are physically separated, with the light-dependent reactions occurring in mesophyll and the Calvin cycle occurring in bundle sheath. First, carbon dioxide in the atmosphere is fixed in mesophyll to form oxaloacetate acid by using phosphoenolpyruvate carboxylase (PEP carboxylase), the non-rubisco enzyme. The oxaloacetate is then converted to malate compound and transported into the bundle sheath. Inside the bundle sheath, malate breaks down and releases carbon dioxide which is later fixed by rubisco and made into sugars in Calvin cycle. Rice, cassava, rubber tree, and palm are C3 plants. On the other hand, sugarcane and maize are C4 plants.

All plants that have chlorophyll used in the photosynthetic process have optimal frequency ranges of light absorbed. Chlorophyll-A plants use 430 nm and 642 nm and chlorophyll-B plants use 453 nm and 662 nm for the most efficient photosynthetic process.

5.2. Temperature

Growth of plants is possible within comparatively broad temperature limits. There are 3 temperature points of growth: minimal temperature for a start of growth, optimal temperature for advantageous growth process, and maximum temperature which stops the growth. In our case, only optimal temperature for growth is considered. Most plants have optimal temperature points for growth vary from 25°C to 28°C but for some plants, the optimal temperature point is slightly higher, especially in C4 plants.

5.3. Humidity and rainfall

Relative humidity is the amount of water vapor in the air relative to the maximum amount. Humidity directly affects when and how plants open the stomata on their leaves. Plants use stomata for respiratory process of them and maintain the amount of water stored in them; thus, the relative humidity of the air in the area is also a significant factor.

6. Data and Software Processing

6.1. Quantitative data

Each Thai economic crop—cassava, maize, palm, rice, rubber tree, and sugarcane—has different suitable ranges of growth which are affected by several growth factors: atmospheric temperature, relative humidity, carbon dioxide intensity, average annual rainfall, red and blue light intensity. AEASat is used to gather these parameters as growth factors of various plants. These factors directly determine the ability to grow in the following environmental condition and during such period.

All 6 growth factors of crops are calculated using correlation coefficient of collected data and ideal data.[4] The ideal data is determined by researching annual yield of each crop for an accurate result. The ideal data for finding correlation coefficient of each crop is given in Table 5.[5,6]

Table 5. Suitability of each economic crop.

Factors	I	II	III	IV	V	VI
Temperature (°C)	29.0	30.0	31.0	26.0	27.0	27.0
Humidity (%)	60.0	82.5	85.0	65.0	85.0	72.5
CO_2 intensity (ppm)	1200	1200	1200	1200	1200	1200
Annual rainfall (mm)	1000	1350	1250	1350	1750	850
Red light (%)	100	100	100	100	100	100
Blue light (%)	100	100	100	100	100	100

As shown in Table 5, crop I, II, III, IV, V and IV are rice, sugarcane, cassava, rubber tree, palm and maize respectively.

They can be numerically analyzed using the suitability equation which is based on correlation coefficient (r):

$$r = \frac{\sum_{i=1}^{N}(x_i - \bar{x})(y_i - \bar{y})}{\sqrt{\sum_{i=1}^{N}(x_i - \bar{x})^2 \sum_{i=1}^{N}(y_i - \bar{y})^2}}. \tag{5}$$

For the numerical manipulation, a mathematical software, MATLAB, is used for this purpose to reduce the calculation time and show the final result as the percentage of suitability of growing each economic crop in the study area. The process of calculation is loading the collected data from study area, calculate the correlation coefficient of each factors; and then find the mean of the coefficients of each crop in percentage and rank which crop is the most suitable of all to effectively and efficiently grow in the area using Relative Suitability Equation, Eq. (6):

$$\mathrm{R.S.} = \left(\frac{1}{6}\sum_{i=1}^{6} r_i\right) \times 100\%\,, \tag{6}$$

while r_i is a correlation coefficient of each factors as Eq. (5).

6.2. Qualitative data

Aside from quantitative data, the qualitative data is also determined. Certain types of data include aerial photograph and crop calendar. The qualitative data cannot be manipulated by numerical or statistical methods but can be considered by using visual interpretation and human logical determination. The AEASat uses Raspberry Pi camera to obtain the individual frame of aerial photograph; and then use an image manipulation software, Microsoft Image Composite Editor to stitch each frame to generate a single merged image as shown in Fig. 6. for an overview of the study area and for determining the feature of topography of the area. For example, if the specific area has residences, that area will not be suitable for growing crops. For interpreting quantitative data and qualitative data, the geographical software, Geographic Information System (GIS) software is primarily used. GIS software is widely used in a geographical field of study by most geographers and cartographers. This software is used to create data maps using interpolation by spatial analysis method. The interpolation method is done by averaging vector information to a rasterized data and overlapping the following data. After overlapping data, those data is categorized by weighing suitability value into 3 categories: highly suitable, moderately suitable, and poorly suitable in each factor. The process of making interpolated maps includes each significant growth factor of overall crops: atmospheric temperature, humidity, carbon dioxide intensity, average annual rainfall by area, pressure, and overall resource overlay—suitability map. Average annual rainfall is extracted from 8 rain gauges around study area and interpolated on the map with GIS software.

Fig. 6. The aerial photograph taken by AEASat in Lop Buri Province, Thailand and processed using Microsoft Image Composite Editor.

6.3. Analysis summary

After the numeric, visual and map analysis is concluded, the report is published on the website of our mission. The point of creating a website for data report is to give an uncomplicated access to a number of agriculturists and farmers. Our website includes introductory, report pages for each study area.

As mentioned, the first launch of AEASat was on December 9th, 2018 in Lop Buri Province, Thailand. The AEASat was descended from the height of 350 meters and performed a safe touch down. The wireless signal was very healthy; only 5 percent of the packets were not complete. We used GIS software to generate a thirty-square-meter- sized interpolated map from collected data to illustrate the efficiency to grow crops of the subarea in the study area as shown in Fig. 7.

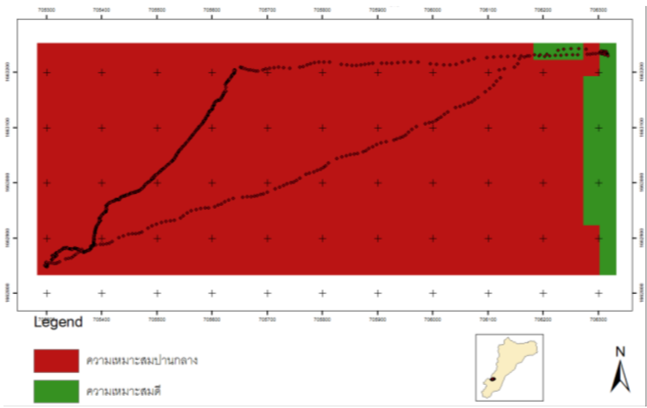

Fig. 7. Interpolated suitability map.

We also used MATLAB to process numerical data and sort the suitability of each crops to grow in the study area. The result of the calculation is given in Table 5 and illustrated with graph in Fig. 8.

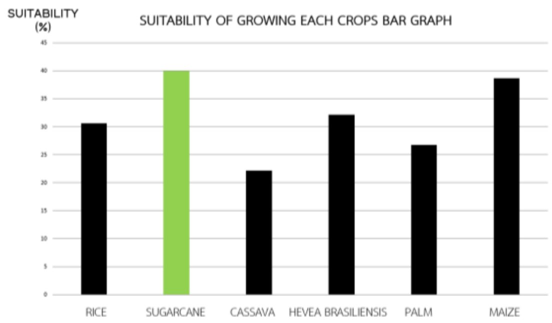

Fig. 8. Result of the calculation shown in bar graph (*Hevea brasiliensis* is another name of rubber tree).

Table 6. Suitability of each economic crop in each factor.

Suitability of factors	I	II	III	IV	V	VI
Temperature (%)	11.78	43.72	9.41	10.56	26.90	38.02
Humidity (%)	39.68	79.16	16.28	46.02	8.72	13.30
CO_2 intensity (%)	56.80	56.80	56.80	56.80	56.80	56.80
Annual rainfall (%)	37.77	67.91	25.60	40.00	10.62	79.42
Red light (%)	79.61	79.61	79.61	79.61	79.61	79.61
Blue light (%)	79.61	79.61	79.61	79.61	79.61	79.61
Overall (%)	50.88	67.80	44.55	52.10	43.71	57.79

As shown in Table 6, it turns out that sugarcane is the most suitable of all economic crops to grow in Lop Buri Province followed by maize, rubber tree, rice, cassava, and palm respectively. The reliability of the result could be confirmed by observing the area around where the AEASat was deployed, we found that most of the crops people grow are sugarcane and maize.

7. System Control and Ground Station

7.1. System overview

The system starts upon the power startup and the AEASat is sent up in the atmosphere to the height of 350 meters. It retrieves the location information from the GPS module and gyroscopic orientation data from gyroscope module; collects parameters: atmospheric pressure, relative humidity, temperature, and carbon dioxide intensity; and then compile the following data into a comma delimited string with identification number as shown in Table 7.

Table 7. Parameter string packets and their size.

No.	Parameters	String sizes in bytes
1.	Counter	1 – 4
2.	Latitude	9
3.	Longitude	9
4.	Altitude	4 – 6
5.	Gyroscopic pitch orientation	4 – 7
6.	Gyroscopic yaw orientation	4 – 7
7.	Atmospheric temperature	5
8.	Atmospheric humidity	5
9.	Atmospheric pressure	7
10.	<Blank byte>	1
11.	<Blank byte>	1
12.	<Blank byte>	1
13.	Carbon dioxide intensity	3 – 4
14.	<Blank byte>	1

When the process is completed, the string will be logged to a microSD card of AEASat; and then wirelessly transmitted to the ground station with LoRa interface protocol. The ground station soon receives the packets from the AEASat. Then LabVIEW shall process strings, classify data, plot coordinates in real time and log data to a CSV file as the aftermath. On the other hand, the ground unit collects parameters: atmospheric pressure, relative humidity, temperature, carbon dioxide intensity, red and blue light intensity and logs data to a microSD card for later post-processing data analysis. The diagram of the system is illustrated as shown in Fig. 9.

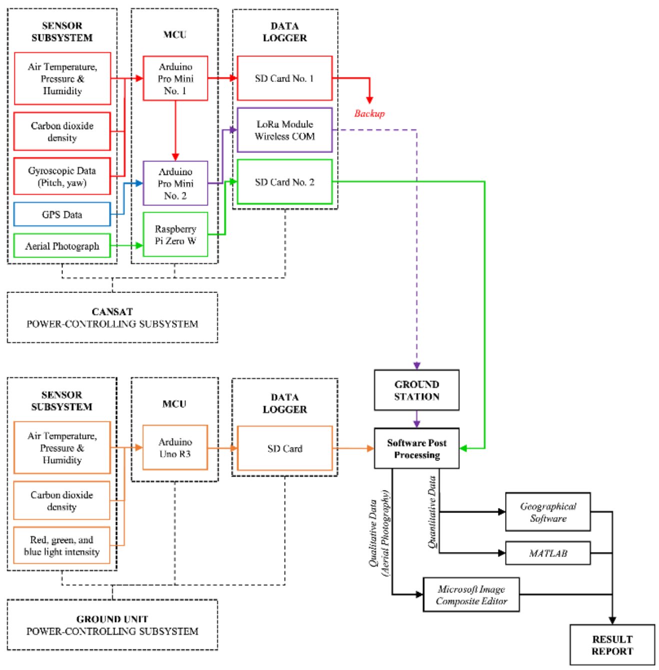

Fig. 9. The block diagram of the system (Arrows represent flowing of data, different colors represent different path of the flow, solid arrow means wired connection and dashed arrow means wireless connection).

7.2. Ground station

The system of our project has two main parts: data-collecting unit—AEASat and ground units, both parts are utilized in C language compiler—and ground station which has different controller interface. The interface which is used on our data-collecting units is hardware control (I^2C, SPI, UART, and LoRa) by which the sensors and LoRa module are connected. On the other hand, the ground station is controlled by a LabVIEW interface, a parallel programming interface. Arduino in the ground station receives data packets which are formatted as comma delimited values from the AEASat using LoRa interface; and then it sends the following data packets through USB port of a computer using serial communication interface.

Using LabVIEW software, the system receives data packets as strings; and then it converts strings into spreadsheet one dimensional array which includes: team ID number, counter, latitude, longitude, altitude, orientational pitch, orientational yaw, atmospheric temperature, humidity, pressure, 2 blank columns, dust intensity, carbon dioxide intensity and a termination character. To prevent receiving unintentional data packets from another team, the team ID number and termination character must match and be case-sensitive. When the data packets are successfully converted and filtered, LabVIEW exports the spreadsheet array as a CSV file and appends new data strings to the old strings every time it receives new data packets until the program termination by user. On the GUI of a program (Fig. 10.), LabVIEW also uses orientational pitch and yaw value to simulate the orientation of AEASat on descent. To visualize the location—using latitude, longitude and altitude—of the AEASat, we embed the Google Earth API to LabVIEW. Google Earth periodically imports the markup-formatted location in comma delimited format using 2 KML files: one for obtaining location from LabVIEW, and one for appending location from the first one to itself and plotting the locations of AEASat on Google Earth in real time. As a result, the AEASat can be tracked while the signal is transmitted, so it is possible to recover the AEASat for reusing in other mission.

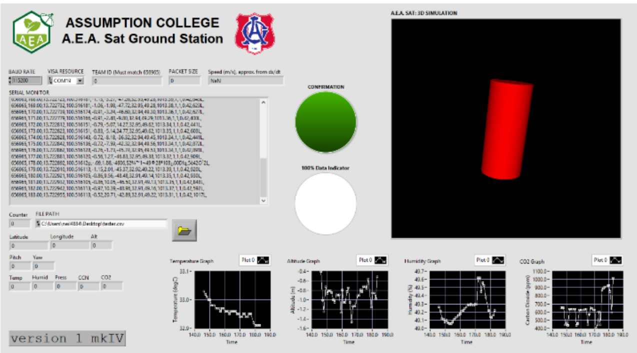

Fig. 10. LabVIEW window interface.

7.3. Hardware subsystem control

As the fact that 1 Arduino Main Controller (MC) cannot handle as many parameters as stated, the system of AEASat uses 2 Arduino Pro Minis along with a Raspberry Pi Zero as MCs. The reason that Arduino Mega 2560 Pro Mini processor board was not used is the oversizing of it, so the Arduino boards were used as 2 MCs to do main task: collecting atmospheric data—temperature, humidity, pressure, dust intensity, and carbon dioxide intensity—receiving GPS coordinates, exporting data packet strings to an SD card and transmitting data packets to the ground station wirelessly. This system uses 3 communication interface protocols—I^2C protocol for using in a wired communication in the connection of BME280, GY-801, CCS811, and one-way communication between 2 Arduino MCs, SPI protocol for communicating with SD card reader module, UART interface (Rx-Tx) for interacting with GPS module to receive GPS coordinates in a proper baud, and LoRa interface for receiving data packets in string and sending them character by character to the ground station for post-processing data analysis. With Arduino MCs, all of the quantitative data is collected and ready for numerical data analysis and the telemetry process is successful. Final model of AEASat is shown in Fig. 11.

Raspberry Pi is also used as third MC for a contrast purpose. As the mission needs aerial photograph to make a visual interpretation for determining the limit of study area. Raspberry Pi has significant advantages over Arduino when a camera factor is considered. The advantages are the support of higher image resolution, faster clock frequency of the hardware, and the stability of the system.

Fig. 11. The final model of AEASat.

8. Conclusion

In this paper, the summary of the agricultural CanSat AEASat model design and development were explained. The missions of AEASat and the satellite system were described, and the data software processing was also mentioned. The detailed mechanical and electronic designs such as enclosure design, parachute design, PCB circuitry, and communication interfaces were explained. From the results and mission evaluation, we were able to improve both mechanical and electronic designs as much as possible. The AEASat satellite model is expected to be improved in terms of compact design, programming interfaces and reduction of control unit of the model, and to be developed for advanced flight mechanism, and the accuracy and precision of software processing method.

The advantage of CanSat is its small size and cylinder configuration. It can be loaded into a rocket and launched over the observation area as a data probe, especially, if the area is very large and inaccessible. As the trajectory and descent path of the rocket and CanSat is calculable regarding wind and other environmental factors, the touchdown position of CanSat and rocket is predictable, thus able to recover from outside said area. The drone is applicable for smaller area, so a CanSat and a Drone has a different methods and purposes of usage.

AEASat can be sent to most rural area for the area exploration and advise agriculturists and farmers to grow the most suitable crops for the most growth efficiency. Finally, they could expect more products and use the area effectively.

Our team enrolled Thailand CanSat Competition 2018. Our deployed CanSat in this competition got The First Place Award and The Best Presentation Award. We can conclude that our process, design, and the result of calculation is reliable and can be used in agricultural process in Thailand.

Acknowledgments

The authors thank all of the people and organizations who supported their CanSat competition participation, funds for making AEASat, MATLAB and LabVIEW software licenses, and AirAsia for sponsoring flight to the symposium. They also appreciate Bro. Dechachai Sripicharn and Bro. Wittaya Thepkom for supporting funds. They especially appreciate Chaowanee Pathomnupong, Saowapa Klinsungnoen and Thanakrit Sulong, teachers of Assumption College, who supported the team at their initiation and Sunthorn Cloth Store Limited for supporting parachute supply. This work is also supported by faculty of Engineering, King Mongkut's Institute of Technology Ladkrabang under the contract number 2562-02-01-023. Finally, the authors thank all the team members who developed CanSat at Thailand CanSat Competition 2018 from other school and competition organizers who manage and host the competition.

References

1) David A. C.: *Fluid Mechanics for Engineers in SI Units,* Pearson Education, New York, 2018.
2) Hugh D. Y. and Roger A. F.: *SEARS AND ZEMANSKY'S UNIVERSITY PHYSICS,* Pearson Education, New York, 2016.
3) James W. H.: *LIGHT AND PLANT GROWTH,* New South Wales, 1988.
4) Unwin H. P. and Roger A.: *Mesoscale Meteorological Modelling.* Academic Press, Inc, Orlando, 1984.
5) Stanford University, https://lagunita.stanford.edu/c4x/HumanitiesScience/StatLearning/asset/linear_regression.pdf (accessed October 20, 2018).
6) Joy T.: *Agricultural Ecology*. Longman, Essex, 1990.
7) U.S. Department of Commerce, National Oceanic and Atmospheric Administration, National Weather Service: National Weather Service Handbook No. 1 – Facsimile Products, Department of Commerce, Washington, DC, 1979.